INTERNATIONAL ATOMIC ENERGY AGENCY
UNITED NATIONS EDUCATIONAL, SCIENTIFIC AND CULTURAL ORGANIZATION
INTERNATIONAL CENTRE FOR THEORETICAL PHYSICS
I.C.T.P., P.O. BOX 586, 34100 TRIESTE, ITALY, CABLE: CENTRATOM TRIESTE

H4.SMR/645-6

SCHOOL ON PHYSICAL METHODS FOR THE STUDY OF THE UPPER AND LOWER ATMOSPHERE SYSTEM

26 October - 6 November 1992
Miramare - Trieste, Italy

Harmonic Analysis of the Seasonal Cycle in Precipitation over the United States:

A comparison between Observations and a General Circulation Model

Sultan Hameed
State University of New York
Stony Brook, NY
USA

Reprinted from JOURNAL OF CLIMATE, Vol. 2, No. 12, December 1989
American Meteorological Society

Harmonic Analysis of the Seasonal Cycle in Precipitation over the United States: A Comparison between Observations and a General Circulation Model

KRISTINA I. KIRKYLA AND SULTAN HAMEED

Institute for Atmospheric Sciences, State University of New York, Stony Brook, New York

(Manuscript received 22 December 1987, in final form 3 July 1989)

ABSTRACT

Using precipitation values obtained from a version of the Oregon State University general circulation model and observational gridded data, harmonic analysis has been employed to study the seasonal variation of precipitation over the conterminous United States. Maps of the first, second and third harmonic amplitudes and phases provide a useful source of comparison between model output and observational data. Results indicate that the method of harmonic analysis allows a more analytical comparison between model predictions and data than the conventional approach of representing the annual march in the form of a curve of mean monthly rainfall amounts. The method delineates regional boundaries of the various precipitation regimes in the United States. The GCM captures a significant amount of the regional detail in precipitation climatology when its results are decomposed by harmonic analysis.

1. Introduction

Precipitation over the United States is governed by a host of physical, spatial and temporal factors. Nestled between the Pacific and Atlantic oceans that exert their own influence upon the land mass, the varying topography and latitudinal extent of the United States also contribute to the nonuniformity of annual precipitation regimes. Precipitation in each region is marked by its own characteristic features and peculiarities associated with the prevailing topographical and atmospheric conditions.

The complexity of precipitation over the United States is intriguing from a climatological perspective, but an understanding of the characteristics of regional precipitation regimes is also of economic and agricultural value. The development of general circulation models (GCMs) has paved the way for innovative climate research; these models can provide a better comprehension of the physical mechanisms of climate. It is therefore important to examine in detail predictions of regional precipitation in GCMs.

Traditionally, comparisons between precipitation simulated in a GCM and observations are made in terms of the geographical distributions of total precipitation for a month or a season (Washington and Parkinson 1986) or in terms of zonal mean values (Potter and Gates 1984). The general conclusion from such comparisons is that most GCMs provide a reasonably satisfactory simulation of the large-scale features of the major rain belts, but do poorly when comparisons are made on regional and local scales. In this paper we present results that show that a GCM can capture details of regional precipitation when seasonal variation is viewed in terms of harmonic components, even though the GCM performs poorly when viewed in terms of conventional criteria such as mean values and total variances.

Harmonic analysis is a particularly useful tool in studying annual precipitation patterns as it reveals the spatial variation of various precipitation characteristics. It delineates the geographic extents of various precipitation regimes and highlights the boundaries between them. The method of harmonic analysis has also been used to investigate seasonal precipitation, by Hsu and Wallace (1976) who discussed global precipitation, and by Hastenrath (1968) who studied precipitation in Central America. A discussion of the method will follow shortly.

The model used in this study is a version of the Oregon State University general circulation model (OSU GCM). The model accounts for two layers in the atmosphere between the surface and 200 mb with internally calculated cloudiness (resulting from either convection or large-scale condensation) and diurnally and seasonally varying radiation; it also has two layers in the ocean, of variable depth, representing a mixed layer and the thermocline (Pollard 1982). The velocity, temperature, geopotential and water vapor mixing ratio are calculated at σ levels, located at the midpoints of the two layers of equal mass. The model also predicts temperature, pressure and surface wetness at ground

Corresponding author address: Prof. Sultan Hameed, Institute for Atmospheric Sciences, State University of New York at Stony Brook, Stony Brook, NY 11794-2300.

level as well as temperature and currents in the two oceanic layers. Topography and surface types are prescribed and are given by Ghan et al. (1982).

The monthly precipitation values for the United States (22°–50°N, 65°–125°W) were averaged over a 23-year integration, producing a dataset of 12 monthly values for each grid location. These values were then subjected to harmonic analysis. A description of the seasonal cycle of precipitation in another version of the OSU GCM (with prescribed sea surface temperatures and sea ice), in terms of zonal mean seasonal anomalies, has been given by Potter and Gates (1984).

The format of our presentation follows the discussions developed by Horn and Bryson (1960) in a paper analyzing the harmonic components of the yearly precipitation over the United States based on monthly means of station observations for a 30-year period, 1921–50. Also included in the discussion will be monthly precipitation values derived from global precipitation data presented by Jaeger (1976) on a 5-degree by 5-degree grid format and, based on climatic atlases and monthly maps from various countries for the time period 1931–60. The data were reconstructed at the Climatic Research Institute of Oregon State University to fit the 4-degree latitude by 5-degree longitude grid format of the OSU GCM, creating a more facile and comparable dataset. Harmonic analysis was employed using the newly gridded values of Jaeger's data and the GCM results.

A source of uncertainty in the comparison is that Horn and Bryson's results are based on data from 1921–50 and those of Jaeger from 1931–60. A discrepancy also arises because of the different horizontal resolution. Horn and Bryson use station data thus providing a fine, although nonuniform resolution. Jaeger's data and the GCM, on the other hand, represent averages on the scale of the grid boxes used. As will be shown later, this coarser resolution leads to the calculation of erroneous phases of the harmonic components in those regions where a transition between regimes occurs. Other differences between the seasonal components of the two datasets will be noted in the following sections.

Figures 1 and 2 respectively display the annual mean (inches/month) and the seasonal variance for each grid point obtained from Jaeger's data and the GCM. A comparison of the simulated and observed values may suggest that the GCM fails to give a consistent account of the regional variations of precipitation over the United States. The results presented in the following sections show that when viewed in terms of harmonic components, however, the GCM does explain significant properties of the regional characteristics of the seasonal precipitation cycle.

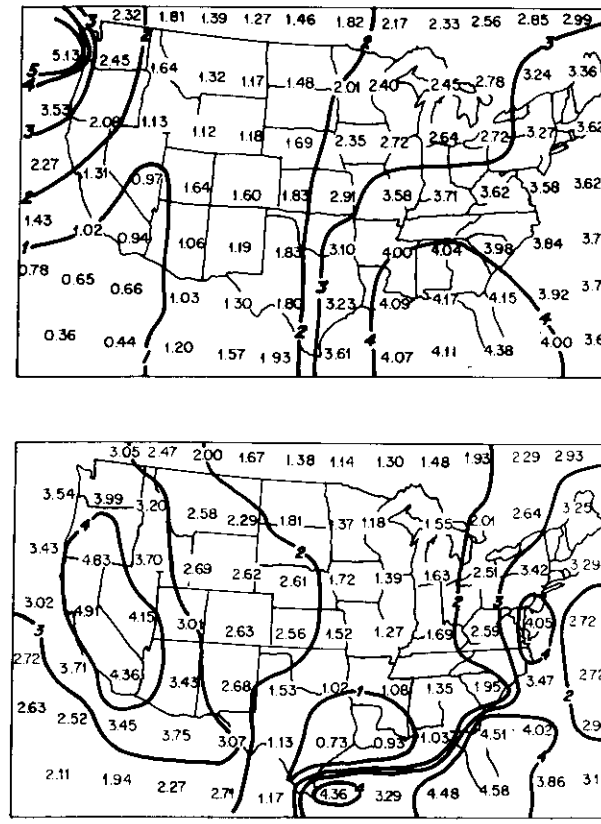

FIG. 1. Annual precipitation means (inches/month) from (a) Jaeger's gridded precipitation data, (b) OSU GCM simulated precipitation values.

2. The method of harmonic analysis

Harmonic analysis is commonly applied to study periodic variations. It is based on the mathematical principle that a curve, viewed as a function, may be represented by a series of trigonometric functions. Simply, the formula for a series is:

$$X = X_0 + \sum_{i=1}^{N/2} A_i \cos\left(\frac{360it}{P} + \Phi_i\right),$$

where X_0 is the arithmetic mean, A_i are the amplitudes of the harmonics, Φ_i are the phase angles of the corresponding harmonics, N is the number of observations, P is the period of observation, and X is the value at time t (Panofsky and Brier 1960). In our case, P is 12 months.

The type of variation dominating the curve is revealed by a comparison of the sizes of the amplitudes, A_i. A large first harmonic amplitude suggests strong annual variation, while a comparatively large second harmonic amplitude points to strong semiannual variation. The phase angle, Φ_i, can be used to determine the time of year the maximum or minimum of a given harmonic occurs.

Although certain harmonics may exert a predominating influence on the curve, often times the annual precipitation march is complicated enough to require

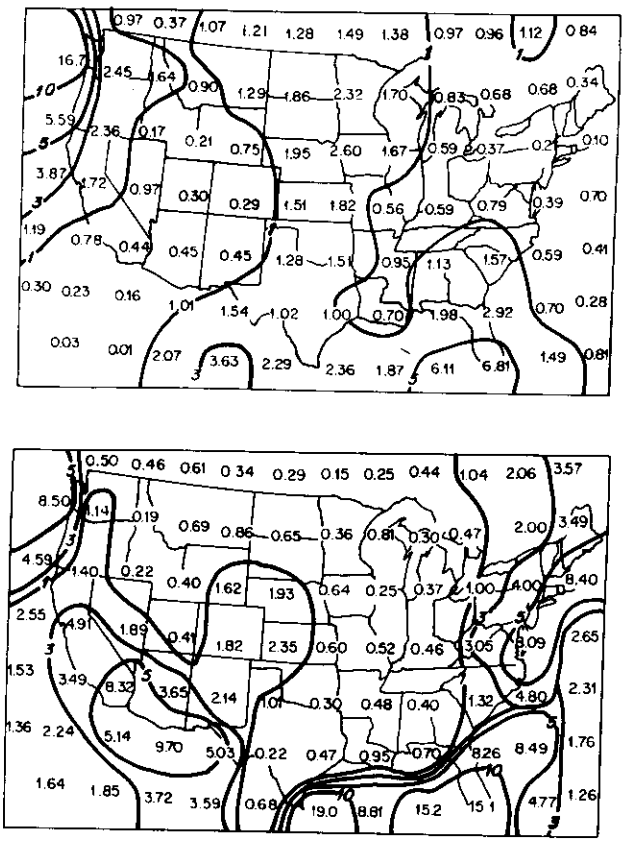

FIG. 2. Sums of squares of the amplitudes of the six harmonics (inches/month)^2 in the annual cycle from (a) Jaeger's gridded data, (b) OSU GCM simulated precipitation data.

the use of all six harmonics. In general, long-period harmonics represent large-scale features of atmospheric circulation while short-period harmonics indicate influences of local phenomena. As will be discussed presently, the method of harmonic analysis helps to delineate and emphasize various boundaries and areas of transition as well as regional characteristics that may otherwise be undetected.

3. Results

a. Contribution of the first three harmonics

The relative contribution from the first three harmonics to the seasonal variance is given by the ratio of the sum of the squares of their amplitudes to the sum of the squares of all six amplitudes. Hence, a ratio value close to unity suggests that the first three harmonics account for most or all of the seasonal variation in the curve; on the other hand, a smaller fraction implies a more complex annual curve with a greater amount of variability contained by the high-frequency harmonics.

Figure 3b illustrates the fraction of total variance contained in the first three harmonics as calculated from model values. The chart indicates that for the western two-thirds of the United States over 90% of the total variability in the seasonal cycle is explained by the first three harmonics, excluding a region over the Rocky Mountains centered about southern Idaho where values decrease to 65%. Jaeger's gridded data (Fig. 3a) reveal a similar pattern, but the region of unexplained variability is more extensive with the first three harmonics accounting for less than 80% of the total variability in precipitation over parts of Idaho, Nevada, Utah and Colorado. Furthermore, over most

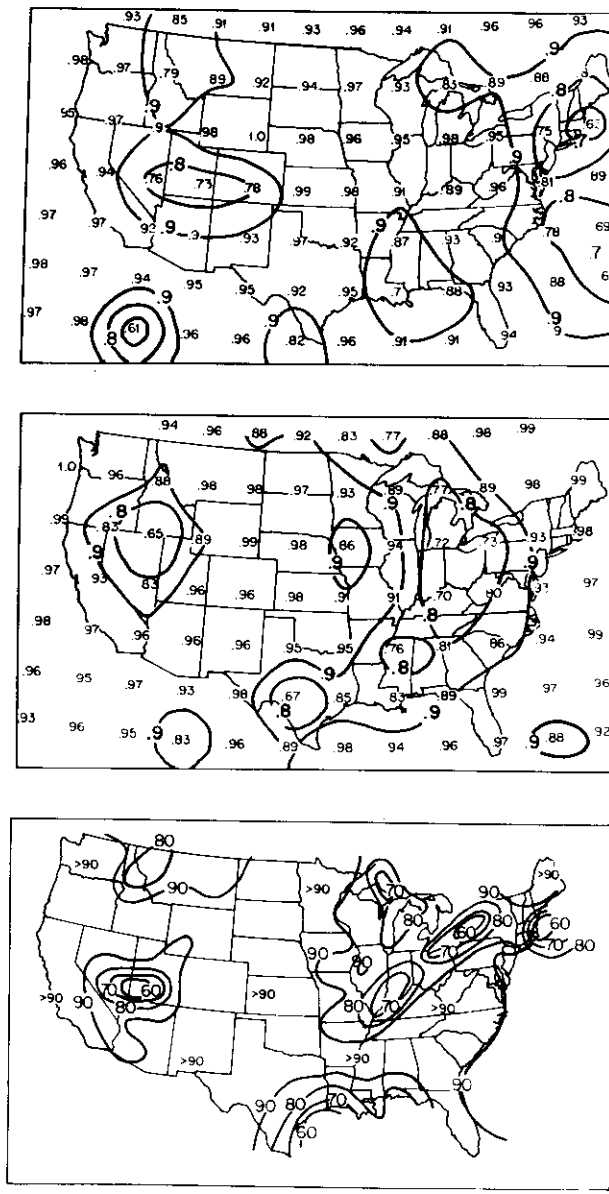

FIG. 3. Percent variability obtained from the first three harmonics of the annual precipitation march from (a) Jaeger's gridded precipitation data, (b) OSU GCM simulated precipitation values, and (c) Horn and Bryson's results.

of the western two-thirds of the country, the fraction of variance is greater than 0.90.

The dominance of the first three harmonics is smaller in the eastern third of the country as their contribution to the total variance decreases. In the GCM (Fig. 3b) from central Texas (67%) northeastward through northern Mississippi and Kentucky approaching the southern Great Lakes region, the percentage of total variability is within the 70%–80% range. Similarly, along the Gulf Coast, and in the southeastern United States values below 90% are found. A region similar in character is found in the gridded data along the northern Gulf coast reaching northeastward into Kentucky (Fig. 3a). These results are in qualitative agreement with those of Horn and Bryson. In the interior southeast portion of the country both the gridded data and Horn and Bryson's results (Figs. 3a, c) show greater contributions from the first three harmonics, while the model shows less (Fig. 3b).

In the GCM results over New England, the first three harmonics explain more than 90% of the total variance of the seasonal cycle. South of the Great Lakes, a decrease in the percent of total variability occurs, and values fall between 70%–80%. Analysis of Jaeger's data provides values of 63% and 75% of total variability over eastern and central New England. Moving northeastward to Maine, Horn and Bryson's analysis shows greater than 90% variability (Fig. 3c), in agreement with the GCM (Fig. 3b), while Jaeger's gridded data reveal a percent of total variability of 80%–90%. Figure 3c also shows two local regions, eastern New England and western New York, where the contribution of the first three harmonics falls to 50% or less. As Horn and Bryson's calculations were performed for specific locations, the distribution of values is more detailed, the contours being more crowded where station data are ample. In contrast, the OSU model and the gridded data yield values that are smoothed and unable to represent local variations within the grid box.

b. The ratio charts

The ratio of the amplitudes of the first and second harmonics is a convenient way of determining the relative importance of these two harmonic components. Figure 4b shows the distribution of the ratio obtained from model results. Two regions of the United States appear to exhibit a dominant influence of the semiannual component (i.e., $A_2 > A_1$): northern Idaho and Washington, and the southeastern part of the country centered over the northern Gulf Coast. Over the remaining parts of the United States, the seasonal precipitation march has a predominant first harmonic, which in some regions is found to be as much as four times the value of the second harmonic. Such regions are found in central California, in the Central Plains, and northern New England.

The feature of two annually dominated regions in the west separated by an area of semiannual influence

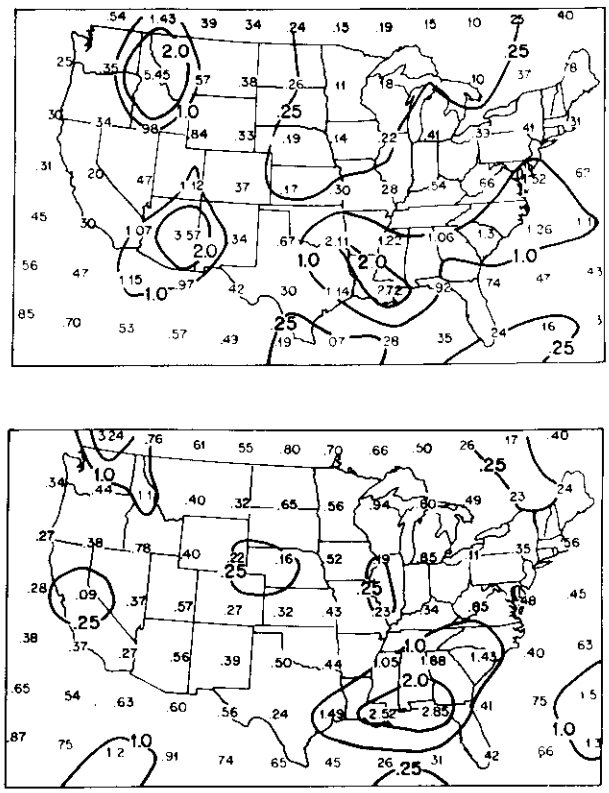

FIG. 4. Distribution of the ratio of the second harmonic amplitude to the first harmonic amplitude (A_2/A_1) from (a) Jaeger's gridded precipitation data, (b) OSU GCM simulated precipitation values.

is more pronounced in the observations. Figure 4a from Jaeger's data reveals the Idaho–Montana region to be one of predominantly semiannual influence ($A_2 > A_1$), as was also noted in the GCM results. However, Fig. 4a also reveals a large area over the Southwest with strong semiannual variation that is not clearly evident in model calculations, although a local maximum of the ratio is observed in this region (Fig. 4b). These regions of greater semiannual variation separate areas of strong annual influence ($A_1 > A_2$) on either side (Figs. 4a, b). East of the Rockies a strong annual harmonic prevails. The expanse of the region where the ratio A_2/A_1 decreases to 0.25 is much greater in Jaeger's data than is observed in model results.

In the southeastern portion of the country, the OSU simulation, which indicates this to be a region of strong semiannual influence ($A_2 > A_1$), is in good agreement with observations. East of the Central Plain states, a separate region characterized by a strong annual harmonic ($A_2/A_1 < 0.25$) is observed in Fig. 4b. A similar region was displayed in Horn and Bryson's ratio chart. In Jaeger's gridded data this region also exhibits a low A_2/A_1 ratio though the region is not separate from the area of strong annual variation found in the Midwest.

Precipitation in the Northeast is influenced most by the annual component of the seasonal cycle. A region

of $A_2/A_1 < 0.25$ is shown by the OSU model reaching northwestward into Canada. A similar region of lower A_2/A_1 ratios is also found in the gridded data (Fig. 4a) but is displaced westward over the Great Lakes.

Horn and Bryson's analysis also revealed several local areas of semiannual dominance ($A_2/A_1 > 1.0$) in the Northeast. The sizes of these features are too small to be resolved by the GCM and gridded data.

c. *The first harmonic phase and amplitude*

The ratio charts helped to emphasize those regions where strong annual or semi-annual variation exists. Figures 5b and 6b show the distribution of the amplitude of the first harmonic, in units of inches, and the corresponding phase given as the month in which it reaches its maximum, as obtained from the model. Large amplitudes are observed in the Pacific Northwest, steadily decreasing to the east and south. Precipitation on the West Coast is maintained by two controlling mechanisms; during the summer a subtropical high pressure cell expands northward and brings dry summers north to the Canadian border, while during the winter the cell shrinks southward and the northern Pacific is dominated by the Aleutian low. Intense and frequent cyclonic storms associated with the southward advance of the polar front shower the West Coast, with precipitation occurring later in winter as the front moves southward. In Fig. 6b of model results, coastal Washington and Oregon and northern California experience a December maximum in precipitation, while the southern California coast shows a January maximum. Over the interior of the western states, amplitudes decrease, suggesting lighter rains, and the period of maxima occurs in late winter and early spring.

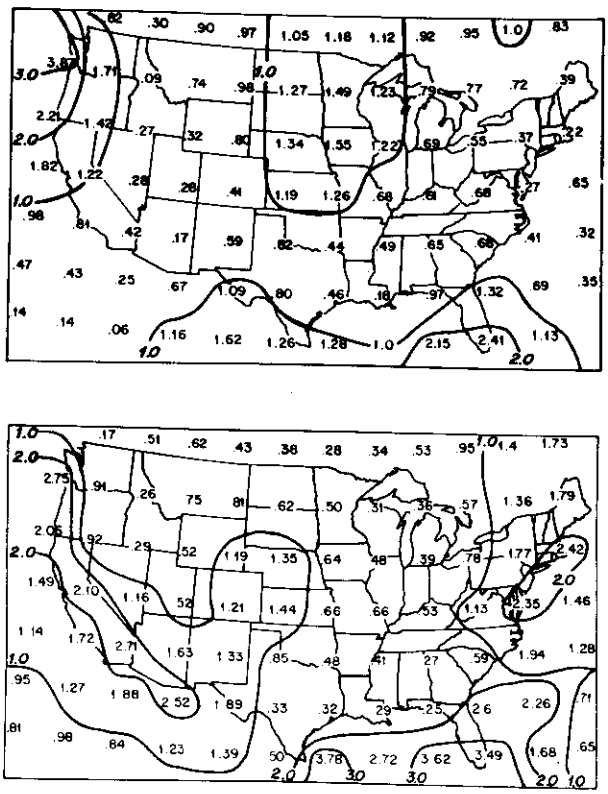

FIG. 5. The first harmonic amplitude (in inches) from (a) Jaeger's gridded precipitation data, (b) OSU GCM simulated precipitation values.

The wide spacing of the isochrones in Fig. 6c of Horn and Bryson's results indicates little variation in the period of maximum, which occurs during winter. The gridded data reveal a similar pattern with heavy December rains in the Northwest, giving way to slightly lighter January rains in California and central Washington and Oregon. First harmonic amplitudes decrease southward and eastward; the weakening rains eastward mark the diminishing effect of Pacific coast climate.

Amplitudes decrease over the Rocky Mountain and intermontane region. The ratio charts indicated that here the second harmonic amplitude exceeds the first harmonic value. This region is one of transition from a Pacific coast climate to a regime characterized by a summer maximum in precipitation. The shift in the time of the first harmonic maximum is evident in Figs. 6a–c. Horn and Bryson's figure shows a phase discontinuity over the northern Rocky Mountain region. Similarly the model results and Jaeger's gridded data, display a shift in the occurrence of the first harmonic maximum. A noticeable feature here is that although the model produces a reasonable representation of the first harmonic maximum to the east and west of northern Idaho (Fig. 6b), it produces a September maximum over northern Idaho; where Jaeger's data point to a February peak in this region. According to the Horn and Bryson figure, the isochrones converge at this location indicating rapidly changing phases; the inconsistency between the model and gridded data is a consequence of the inability of either to represent the rapidly shifting phase within the grid boxes in a transition region.

Moving eastward across the mountains, the tendency for a summer maximum in precipitation becomes stronger. The interiors of continents in the midlatitudes have a pronounced summer maximum, as the greater influx of moisture and convective activity during the summer outweighs the cyclonic turbulence during the winter season. East of the Rockies the annual harmonic is again dominant.

Figure 6b, which displays the occurrence of the maximum of the annual harmonic for the OSU model, shows a transition southeastward from a July maximum in central Montana and Wyoming to a June maximum, reaching New Mexico in the south and western Kansas and Nebraska in the east. North Dakota appears to have a May maximum. Where strong annual variation exists, amplitude values are greater.

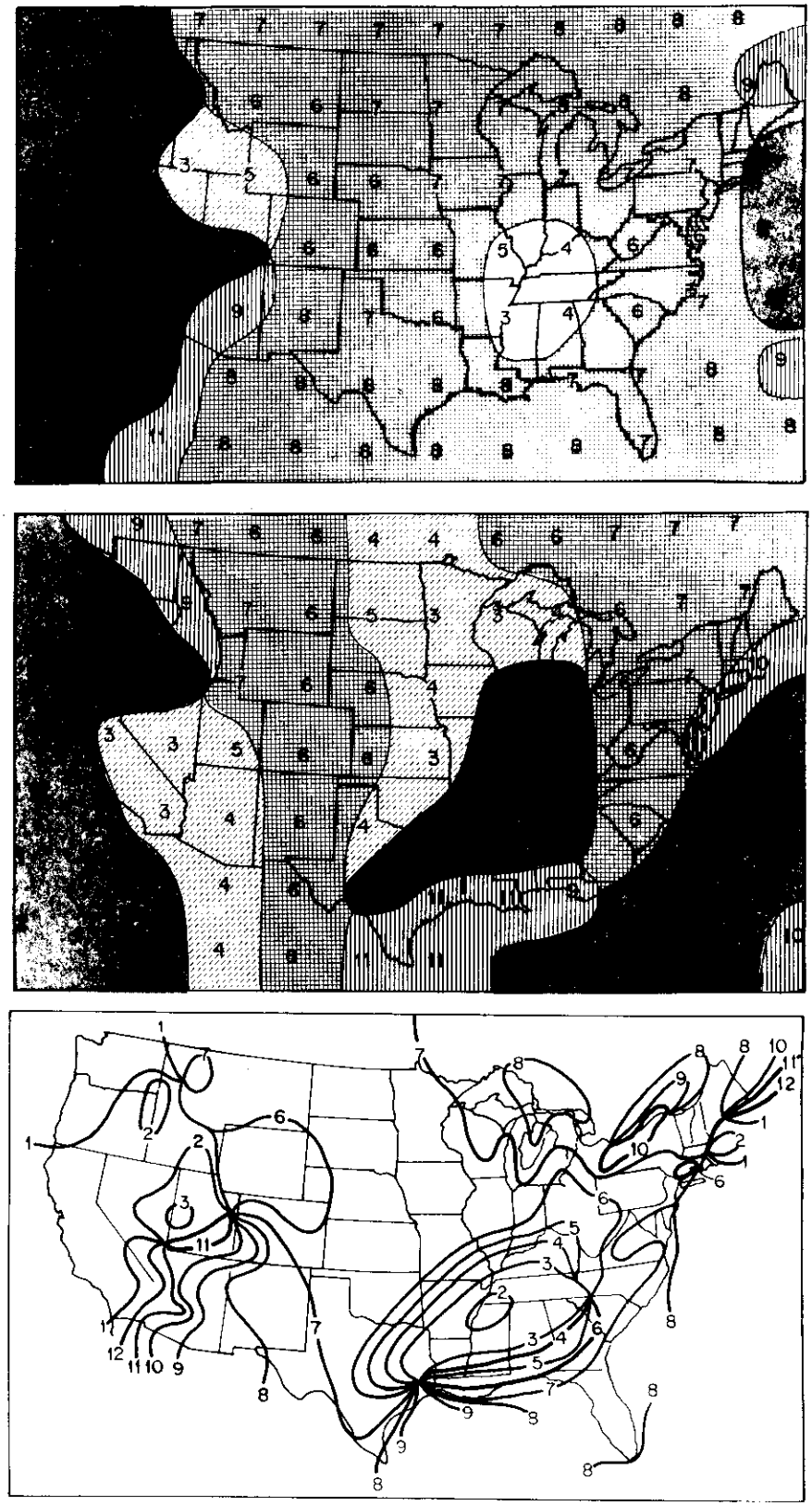

FIG. 6. The phase of the first harmonic is shown by the month in which the maximum value occurs for (a) Jaeger's gridded precipitation data; the four seasons are identified by different shadings (December, January and February represent winter, etc.), (b) OSU GCM simulated precipitation values; the four seasons are identified by different shadings, (c) Horn and Bryson's results based on station data.

The amplitude chart (Fig. 5b) reveals that the annual characteristic is most developed over eastern New Mexico and Colorado, and Nebraska and Kansas.

Figure 6a reveals the month of first harmonic maximum obtained from the gridded data. Here, a May maximum in western Wyoming changes rapidly northward to a June maximum both in Montana and southeastward through eastern Wyoming, Colorado, Nebraska and Kansas. A July maximum is found over the Dakotas, Minnesota, Wisconsin and Iowa. Highest amplitudes of the first harmonic are found over Iowa, Nebraska and Minnesota, contrary to model results where largest amplitudes are observed over the Central Plain states. The expanse of the region of summer maximum (June, July, August) is smaller in the model, not reaching as far eastward as in Horn and Bryson's and Jaeger's gridded data.

Horn and Bryson's diagram of the first harmonic amplitude shows a sharp gradient of amplitude from Kansas decreasing to a minimum in Arkansas, followed by an abrupt increase to a local maximum in Mississippi. This region is also one of rapid transition in phase. This regime has been labeled "Tennessee-type" and is characteristic of the area extending from central Mississippi into northeastern Tennessee. Late winter and early spring rains result from the position of the jet stream during this time of year and the passage of cyclonic storms.

Because of the lower spatial resolution in the gridded data, this feature is not as developed in Figs. 5a and 6a of Jaeger's data, although local minima in amplitude exist over Arkansas and Mississippi. It can also be noted that Texas shows a relatively rapid shift from an August maximum in central Texas to a June maximum in the northeastern part of the state, replaced by a March maximum in Arkansas and Mississippi. However this region, unlike Horn and Bryson's observations, is dominated by the semiannual harmonic, and the rapid change in phase may suggest a transition in precipitation regimes.

Figure 5b, which shows model results, reveals a sharp decrease in first harmonic amplitude between Kansas and the southeastern portion of the country. A sharp transition in the period of maximum occurs, as was also noted in Jaeger's data, although the distribution of the first harmonic maximum in the model results is not accurate. This inconsistency may be a consequence of the pronounced semiannual variation produced by the model in this region east of Texas.

The Northeast is characterized by a strong annual term in the model. Amplitude values along the Atlantic coast, however, are small in the gridded data. Figure 6a shows a discontinuity in the first harmonic maximum along the coast, revealing the difference between the interior precipitation regime with a July maximum and the coastal regime with a December maximum. This observation is also made by Horn and Bryson (1960). Figure 6b, displaying the first harmonic maximum obtained from model results, reveals a similar distribution with the interior showing a July maximum, but the coastal region has an October maximum. Once again, it is difficult to categorize the time of maximum in a region where the phase shifts rapidly, so that the values observed in Jaeger's data and in the model are not properly representative. We also note that the amplitude of the first harmonic along the coast is greater than the amplitudes in the interior. Quick inspection of the ratio chart (Fig. 4b), however, reveals a larger ratio in this region, and therefore little difference between amplitude values of the first and second harmonics. In general, over much of the Northeast, all six harmonic terms are small in the observations, with little variation in monthly precipitation.

Finally, Fig. 6c, which displays the first harmonic phase calculated by Horn and Bryson, shows a discontinuity along the Great Lakes region. To the west and north of Lake Erie and Lake Ontario a summer maximum is noted; but, along the southeastern shores, the maximum shifts to late fall. This feature is not noted in either the gridded data or the model results, due to the lack of resolution. An observed July–August maximum in the gridded data and a June–July maximum in the model is revealed for this region.

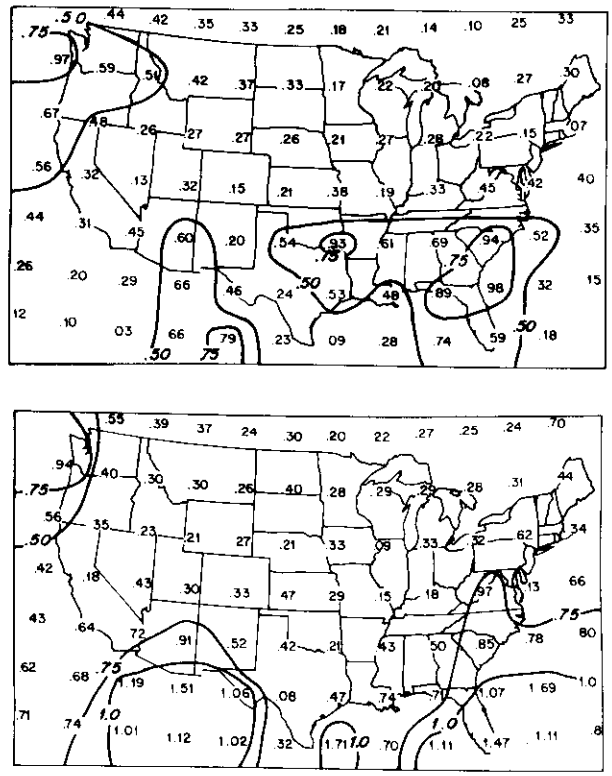

FIG. 7. The second harmonic amplitude (in inches) from (a) Jaeger's gridded precipitation data, (b) OSU GCM simulated precipitation values.

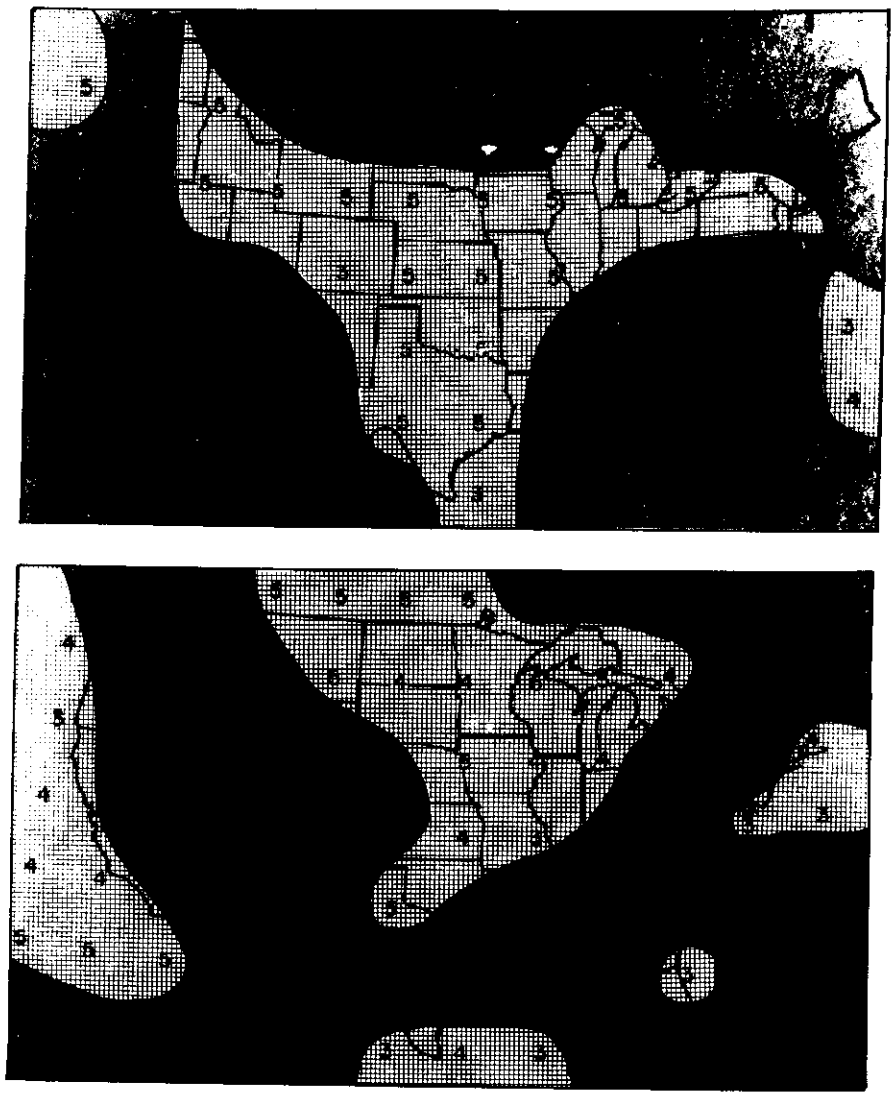

FIG. 8. The phase of the second harmonic is shown by the month in which the maximum value occurs. Another maximum occurs six months after the month indicated. Regions where the second harmonic maximum occurs in summer and winter are shaded dark, the other regions are characterized by maxima in spring and fall: (a) Jaeger's gridded precipitation data, (b) OSU GCM simulated precipitation values.

d. The second harmonic phase and amplitude

The model ratio chart (Fig. 4b) reveals strong semiannual variation over northeastern Idaho and western Montana. Here, the region exhibits June and December maxima (Fig. 8b) which actually occur a month later than the gridded observational data. The second harmonic amplitude obtained from the GCM over this region (0.30) compares well with Horn and Bryson's calculated values, 0.2–0.4, although it is slightly smaller than the value obtained from Jaeger's gridded data (0.51). As was mentioned in the previous section, the northern Rocky Mountain region marks the transition between the Pacific type and continental precipitation regimes. Interestingly, the second harmonic maxima are more or less concurrent with the first harmonic maximum on either side of this boundary feature.

A large area of dominant semiannual variation was noted over the southern intermontane region in Fig. 4a of the gridded data. The phase discontinuity in Fig. 8a delineates the northern boundary of this precipitation feature, lying east–west across Utah and Nevada. The region south of the discontinuity is marked by February and August maxima. This semiannual effect is most pronounced in Fig. 7b across the Arizona–New Mexico border. This feature has been labeled the "Ar-

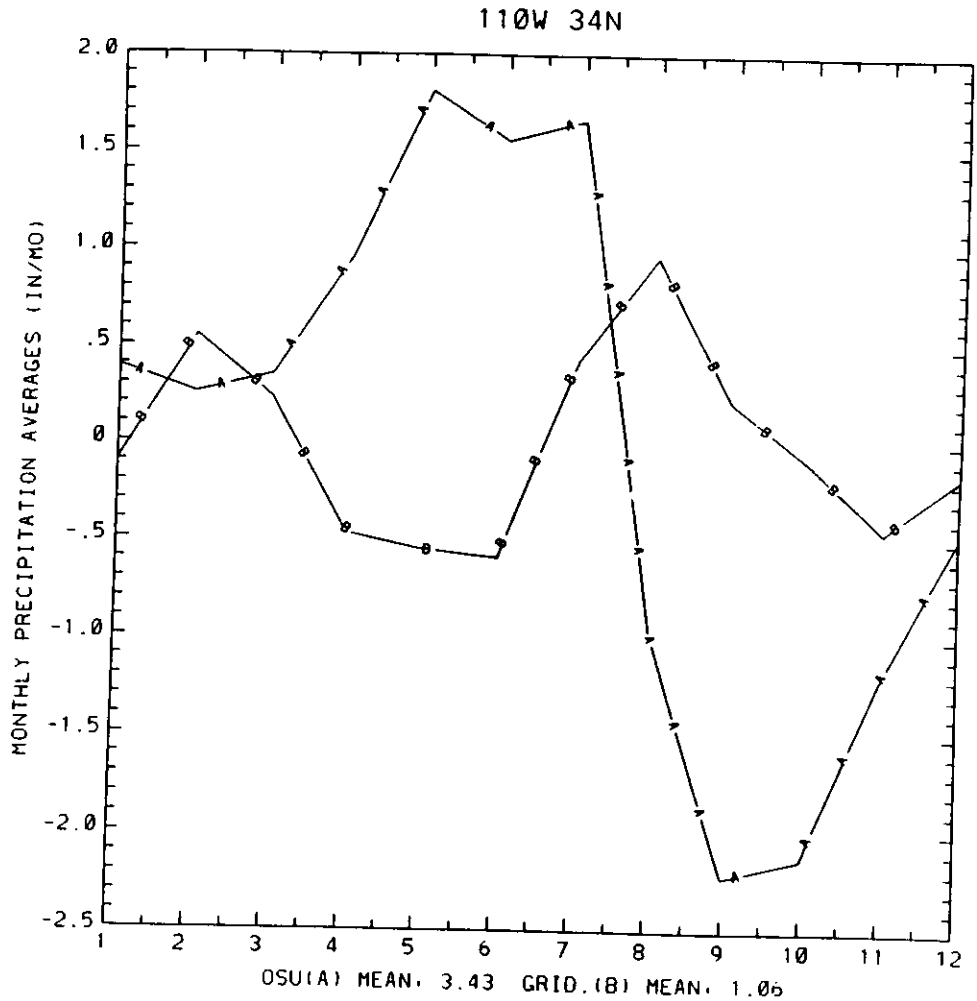

FIG. 9. Average monthly precipitation and yearly means (inches/month) for 110°W, 34°N (eastern Arizona) for (a) OSU GCM simulated precipitation values, and (b) Jaeger's gridded precipitation data.

izona-type" precipitation pattern and is unique because two different precipitation controls affect the rainfall in this region. Winter precipitation occurs as Pacific storms advance eastward, while summer showers arise from a singularity in air flow that permits precipitation to increase suddenly (Lydolph 1985). These two wet periods are separated by a dry spell in late spring and early summer. A rapid phase transition is noted over eastern New Mexico and western Texas (Fig. 8a) delineating the eastern boundary of this precipitation regime; but second harmonic amplitude values are comparatively small (Fig. 7a) and although the semiannual tendency exists in New Mexico, it is masked by a dominant annual term. The Arizona-type semiannual precipitation pattern was undetected in model results (Fig. 4b), although the ratio A_2/A_1 shows a local maximum in this region. Figure 9, displaying the yearly precipitation march for the model and gridded data, shows the two-season pattern in the gridded data curve B. Furthermore, it appears that not only did the model overestimate the yearly variation, but the annual mean as well.

According to the ratio charts (Figs. 4a, b) the area of the northern Gulf Coast and northward, experiences dominant semiannual variation. The gridded data show February and August maxima occurring in Florida shifting to early summer and early winter maxima over Louisiana and Texas. The semiannual term is most pronounced from northeastern Texas to South Carolina (Fig. 7a). The model produces February and August maxima all along the northern Gulf Coast, with largest amplitudes observed over northwestern Florida. In the model semiannual variation is most pronounced over South Carolina with maxima occurring in January and July. Horn and Bryson's analysis also revealed a small region of semiannual dominance over northeastern Georgia and western South Carolina with midsummer and midwinter maxima. In both the model

and gridded data, the regions where $A_2/A_1 > 1.0$ appear to be smeared across a much larger area of the southeastern portion of the country (Figs. 4a, b).

e. *The third harmonic amplitude and phase*

The third harmonic describes those maxima that have a tendency to occur four months apart. Figures 10a, b reveal the third harmonic amplitudes, and Figs. 11a, b illustrate their respective phases, for Jaeger's data and the model. The largest third harmonic amplitude values are observed off the southeastern coast of Texas in both the model and gridded data, similar to the observations made by Horn and Bryson. A value of 1.2 inches is observed for the OSU model, which is comparable to Horn and Bryson's calculated value. However the model produces a first harmonic amplitude that is erroneously high (3.78), underestimating the relative contribution of the third harmonic. The gridded data reveal an amplitude of 0.78, which (although a local maximum) is also small in comparison with the amplitude of the first harmonic (1.28). The model experiences maxima in February, June and October in this region, with the October maximum concurrent with the first harmonic peak. The gridded data

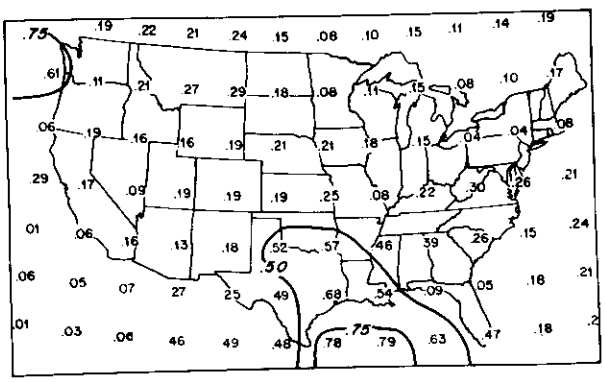

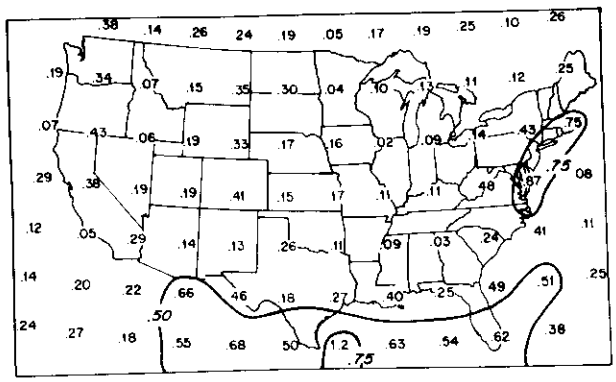

FIG. 10. The third harmonic amplitude (in inches) from (a) Jaeger's gridded precipitation data, (b) OSU GCM simulated precipitation values.

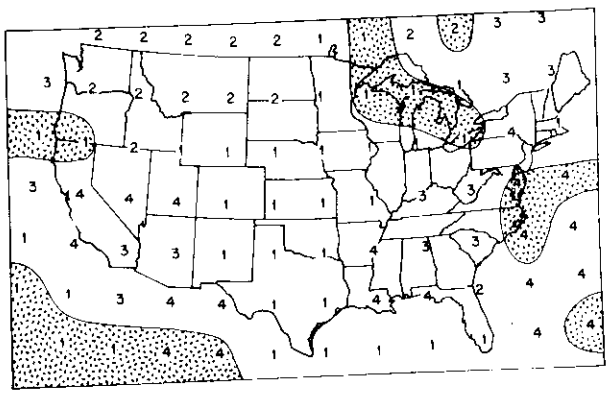

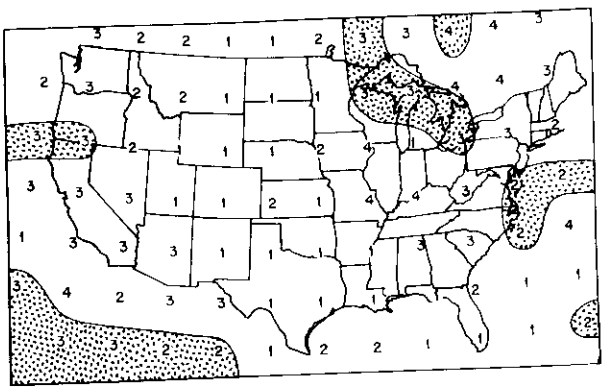

FIG. 11. The phase of the third harmonic is indicated by the month in which the maximum value occurs. Two other maxima occur four and eight months after the month shown. (a) Jaeger's gridded precipitation data, (b) OSU GCM simulated precipitation values. Regions where the third harmonic phases in Jaeger's data and the GCM differ by more than a month, are shaded.

reveal January, May, and September maxima, the last being coincident with the first harmonic maximum.

In Fig. 10b of the GCM results, the southeastern tip of Florida contains an amplitude of 0.62, with maxima occurring in January, May and September. Jaeger's gridded data produce a lower amplitude of 0.47 (Fig. 10a) with maxima occurring in the same months as the GCM. Horn and Bryson's figures reveal the region as having third harmonic amplitudes much larger (2–4 inches) than those for model and gridded data with maxima occurring in February, June and October.

f. *Some local phenomena*

The results of harmonic analysis discussed above enable us to distinguish different precipitation regimes and transition regions. Several regions characterized by relatively low contributions from the first three harmonics were also identified. In such regions the higher harmonics, often representing local-scale phenomena, are more prominent. Further investigation of such areas leads us to identify regimes characterized by unusual seasonal patterns. We give two examples.

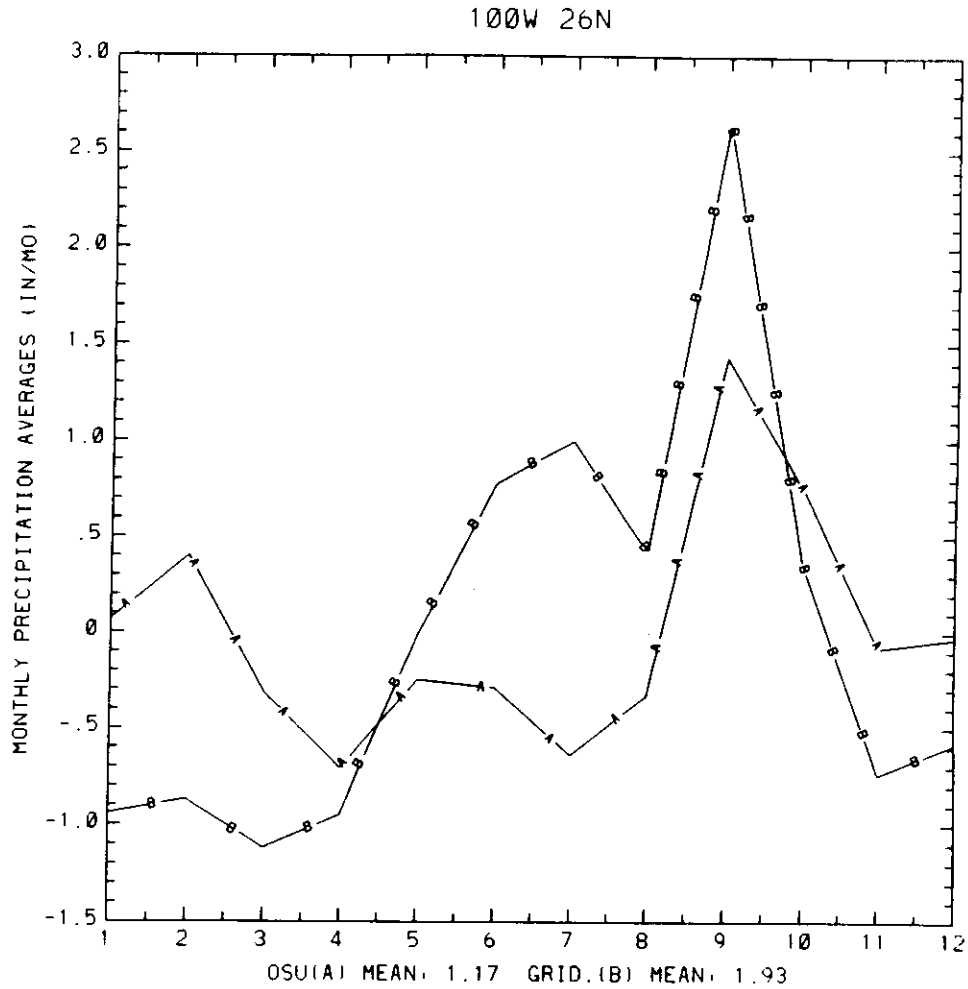

FIG. 12. Average monthly precipitation and yearly mean (inches/month) for 100°W, 26°N (Mexico) for (a) OSU GCM simulated precipitation values, and (b) Jaeger's gridded precipitation data.

The percent variation contained in the first three harmonics falls below 70% over central Texas in both the model and gridded data (Fig. 3a, b). This corresponds to a climatic peculiarity occurring in Texas causing a midsummer minimum in precipitation associated with the development of a high pressure ridge and a dry tongue of air extending northeastward through the midsection of the continent (Lydolph 1985). This particular feature is found to occur in Texas and southward into the western fringes of the Caribbean and eastern Mexico. Plotted on Fig. 12 are the monthly precipitation values (mean subtracted) for the grid box at 26°N, 100°W. At this location, the gridded data show a minimum in August, while the model produces a July minimum.

The Ohio River valley, from southern Illinois northeastward through Pennsylvania shows a tendency for alternate increases and decreases in monthly precipitation. In the model, the first three harmonics account for 80% of the total variation in the annual precipitation curve. A noticeable feature in this region is that October is the driest month of the year, reflecting the annual occurrence of "Indian Summer"—clear, mild, hazy weather due to the stagnation of a high pressure cell over the Appalachian region during this time of year. The October minimum is evident in Fig. 13 of the annual trend of Jaeger's gridded data in northern central Kentucky. The model also produces this feature at this and neighboring locations.

4. Concluding remarks

The complexity of precipitation climatology over the United States stems from topographical and atmospheric variations, which in turn influence local and regional precipitation regimes. Conventionally, precipitation data have been viewed in the form of monthly averages. Our results show that harmonic analysis permits a more detailed investigation of the seasonal cycle because it decomposes the annual march

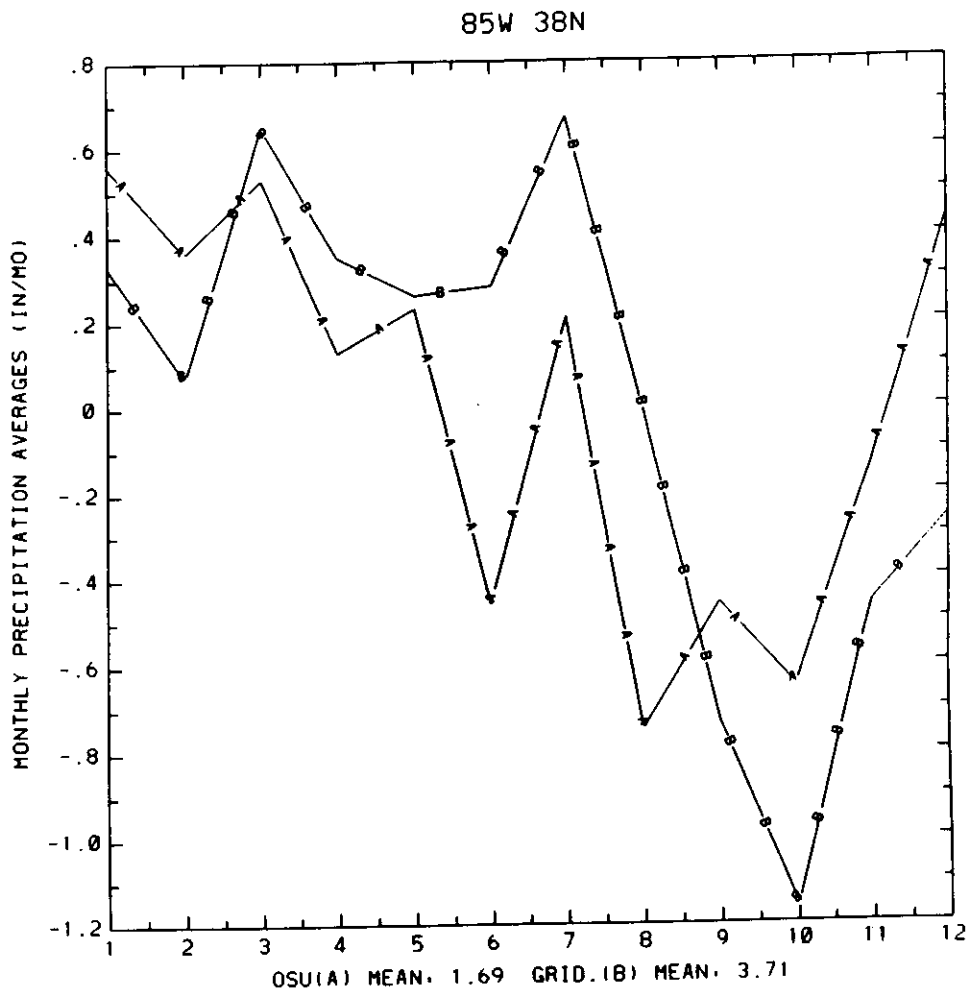

FIG. 13. Average monthly precipitation and yearly mean (inches/month) for 85°W, 38°N (central Kentucky) for (a) OSU GCM simulated precipitation values, and (b) Jaeger's gridded precipitation data.

into independent terms that describe long or short term variations. Harmonic analysis permits an objective approach to the study of climatological features. It distinguishes regional and local characteristics as well as delineating boundaries between precipitation regimes.

The comparison between simulated precipitation values of the GCM and observational data has proven both informative and fruitful. Results indicate that the OSU GCM reproduces many regional and local precipitation features in convincing detail. The model distinguishes between Pacific coast and continental precipitation regimes with their respective winter and summer maxima. Regions with strong annual or semiannual tendencies are delineated fairly accurately. The strong annual variation apparent over the immediate West Coast and over the Central Plain states is evident in model results. Similarly, the semiannual tendency found in the region of the Gulf Coast and over the northern intermontane region is also present in model simulated values. The model sometimes fails to reproduce local phenomena, such as the Arizona-type precipitation pattern seen in the observational data, but the model reproduced other local features like the Indian Summer in the Ohio valley and the midsummer precipitation minimum in southern Texas.

The local features are associated with local topographic and atmospheric conditions whose effects are noticeable in the higher harmonics that describe small-scale patterns. Conversely, the first, second and sometimes third harmonics explain characteristics that are more expansive by nature. Evaluating the discrepancies between harmonic values of model and observational data may provide useful information on the ability of the model to reproduce atmospheric phenomena on different temporal and geographical scales.

Acknowledgments. This work was performed under the auspices of the CO_2 Research Division, Office of

Basic Energy Sciences, U.S. Department of Energy. We thank Drs. G. L. Potter and W. L. Gates for making available the results of the Oregon State University general circulation model, and Dr. Richard Rosen for his editorial contributions.

REFERENCES

Ghan, S. J., J. W. Lingas, M. E. Schlesinger, R. C. Mobley and W. L. Gates, 1982: A documentation of the Oregon State University two-level atmospheric general circulation model. Report No. 35, 395 pp. [Available from Climate Research Institute, Oregon State University, Corvallis.]

Hastenrath, S. L., 1968: Fourier analysis of Central American rainfall. *Arch. Meteor. Geophys. Bioklim.*, **B16,** 81–94.

Horn, L. H., and R. A. Bryson, 1960: Harmonic analysis of the annual march of precipitation over the United States. *Ann. Assoc. Amer. Geogr.*, **50,** 157–171.

Hsu, C. F., and J. M. Wallace, 1976: The global distribution of the annual and semiannual cycles in precipitation. *Mon. Wea. Rev.*, **104,** 1093–1101.

Jaeger, L., 1976: Monatskarten des Niederschlags Für die ganze Erde. *Ber. Dtsch. Wetterdienstes* **18,** No. 139, 38 pp.

Lydolph, P. E., 1985: *The Climate of the Earth.* Rowan and Allanheld, 202–246.

Panofsky, H. A., and G. W. Brier, 1960: *Some Applications of Statistics to Meteorology.* The Pennsylvania State University, 128–134.

Pollard, D., 1982: The performance of an upper-ocean model coupled to an atmospheric general circulation model: Preliminary results. Report No. 31, p. 32. [Available from Climatic Research Institute, Oregon State University, Corvallis.]

Potter, G. L., and W. L. Gates, 1984: A preliminary intercomparison of the seasonal response of two atmospheric climate models. *Mon. Wea. Rev.*, **112,** 909–917.

Washington, W. M., and C. L. Parkinson, 1986: *An Introduction to Three-Dimensional Climate Modeling.* University Science Books, 222–223.